**Title:**

# RecBCD possesses strong coupling between DNA and nucleotide binding that may propel a stepping mechanism during translocation.

Authors:

Vera Gaydar, Rani Zananiri, Or Dvir, Ariel Kaplan and Arnon Henn*

Faculty of Biology, Technion - Israel Institute of Technology, Haifa, 3200003, Israel

*To whom correspondence should be addressed:

AH: Tel. +97248295424; Fax. +97248295424; Email: arnon.henn@technion.ac.il

Key words: RecBCD, Helicase, Nucleotide-Binding Linkage, Thermodynamic Coupling

*Specific contributions*: VG, RZ, AK & AH designed, performed research, analyzed data and wrote the paper. OD performed research.

**Abstract**

Double strand breaks are the severest genomic damage requiring rapid repair response. In prokaryotes, members of the RecBCD family initiate DNA unwinding essential for double strand break repair mechanism by homologous recombination. RecBCD is a highly processive DNA helicase with an unwinding rate approaching ~1,600 $bp \cdot s^{-1}$. The ATPase reaction mechanism enabling RecBCD to achieve this fast unwinding rate and its enzymatic adaptation are not fully understood. Here, we present thermodynamic investigation of DNA and nucleotide binding to RecBCD to reveal the binding linkage and the degree of coupling between its nucleotide cofactor and DNA substrate binding. We find that RecBCD exhibits a weak binding state in the presence of ADP towards double overhang DNA substrate (dohDNA), and the same degree of coupling is observed for RecBCD affinity toward ADP, only in the presence of dohDNA. In the absence of nucleotide cofactor (APO state) or in the presence of AMPpNp, much weaker coupling is observed between the binding of DNA and the nucleotide state towards RecBCD. Other DNA substrates that are not optimally engaged with RecBCD do not exhibit similar degree of coupling. This may be the first evidence for strong and weak binding states that can, in principle, regulate a 'stepping mechanism' during processive translocation of RecBCD.

## Introduction

Double Strand Breaks (DSBs) in the genome are the severest damage in DNA of all kingdoms of life. Helicases play an essential role in the repair mechanisms for DSBs in every living organism. In prokaryotes, members of the RecBCD family initiate unwinding of DSBs in preparation for strand invasion which is essential for repair by homologous recombination [1]. RecBCD is a highly processive DNA helicase exhibiting an exceptionally high unwinding rate of ~ 1,600 base pairs (bp) per second ($s^{-1}$) [2]. RecBCD is a heterotrimer composed of one copy of each of the DNA translocases and helicases namely, RecB, RecC, and RecD [3, 4]. The RecC subunit "staples" the RecB and RecD subunits [5], and plays a crucial role in destabilizing the duplex DNA ahead of the translocases activities of RecB and RecD unwinding [5], and in recognition of the Chi sequence [6, 7]. RecBCD utilizes ssDNA translocation on opposite DNA polarities with RecB moving on the 3' - 5' strand and RecD moving on the 5' - 3' strand with overall net translocation of RecBCD complex along the duplex DNA [4, 8-10]. Although the repair mechanisms of DSBs are found in all living organism, there is no known eukaryotic homologous of RecBCD in terms of its structural organization or rapid and processive unwinding.

For RecBCD to transverse processively with the two motors translocating along the single strands of the DNA, a stepping-like mechanism is most likely required. For net vectorial translocation, a simple alternation between strong and weak DNA binding states can provide such mechanism of stepping [11-13]. Threading through ssDNA channels still must be via alteration between attached (strong binding state) to detached states (weak binding states). In this sense, RecBCD can be viewed as a double headed ATPase molecular machine, i.e., a molecular motor that has two motors that transverse along the DNA lattice. This is highly analogues to a

molecular motor such as myosin V whereas its processive stepping along the actin filament can be describe by walking hand over hand [14]. Threading ssDNA through semi open DNA tunnel that form in RecB, and partially in RecD, will increase processivity but will still be requiring cycles of coordinated association-dissociation transitions to permit net vectorial translocation. The basis for this long-distance stepping motility lays in the specific nucleotide state/s that modulate the affinity towards the lattice between strong and weak affinities, allowing the motor to dissociate and re-associate with respect to the lattice [15]. However, the thermodynamic basis for the strong and weak nucleotide states during translocation has not yet been resolved for RecBCD. Therefore, identifying the existence of such intermediates during the mechanochemical ATPase cycle is important to understand how RecBCD may perform its processive and rapid translocation. The bound nucleotide state (ATP, ADP·$P_i$, or ADP) modulates the motor affinities towards the lattice it transverse on, as has been shown for all myosins, kinesin as well as for some helicases [16-20]. For RecBCD this has not yet been determined systematically with DNA substrate with respect to the nucleotide state.

In this work, we characterized RecBCD's binding to diverse DNA substrates and nucleotides mimicking intermediate states along its reaction cycle to reveal nucleotide binding linkage within RecBCD. We show that RecBCD and RecBCD·DNA·nucleotide complex exhibits weak coupling between the nucleotide and the DNA bound to RecBCD complexes exhibit in most states, whereas it exhibits a strong coupling in a single unique state. Specifically, we found that RecBCD·ADP complex exhibits weak affinity towards dohDNA (~40-fold reduction), unlike any other state or DNA substrate. The opposite is also true in which RecBCD· dohDNA exhibits much weaker affinity towards ADP. This may present one state in which strong coupling between dohDNA and ADP binding is observed. The AMPpNp state weakens the

affinity towards the 3ohDNA by 2- fold while the ADP strengthens the affinity of 3ohDNA substrate towards RecBCD by ~5-fold (Fig. 1D & 1E). Since dohDNA shows the strongest impact to modulates nucleotide affinity and vice versa, we propose that such strong coupling must be mediated via multiple DNA contact sites. In contrast, partial DNA overhang DNA substrates don't show such impact on modulating the affinities of RecBCD. Long range communication may exist between the subunits during translocations to facilitate strong to weak binding transitions.

## Results

### RecBCD oligomeric state and DNA stoichiometric binding

We examined the nucleotide binding linkage of RecBCD by performing equilibrium binding assays of DNA substrates in the absence and presence of AMPpNp and ADP. For this we have devised a set of DNA substrates that can mimic three major states engaged with RecBCD, initiation (hpDNA), translocation (ssDNA), and unwinding and translocation with overhang on both 5' and 3' (dohDNA), and two additional substrates with either 5' or 3' ohDNA engaged with RecD or RecB, respectively [5, 21] (Fig. 1, Table 1). To measure DNA and nucleotide binding linkage with respect to RecBCD complex, the oligomeric state in solution of RecBCD under our experimental conditions must be determined, similarly to what has been performed that ruled out the existence of a dimer of RecBCD during catalysis [7]. Figure 2 shows the stoichiometric binding of ssDNA and hpDNA (Fig. 1, Table 1) under the condition in which [DNA] >> $K_D$ and RecBCD is titrated well above the $K_D$ (Fig. 3, Table 2) measured by Fluorescence Anisotropy (FA) (Fig. 2A) and fitted according to Equation 1:

$$[RecBCD \cdot DNA] = \frac{\left(R + n + \frac{K_D}{[DNA]_T}\right) + \sqrt{\left(R + n + \frac{K_D}{[DNA]_T}\right)^2 - 4R \cdot n}}{2n} \quad \text{(Eq. 1)}$$

Under stoichiometric conditions of $[DNA]_T >> K_D$, R is the plotted (experimental) mole/mole ratio of RecBCD/DNA and n is the ratio of the fit of RecBCD to DNA, and the $DNA_T$ is the DNA (ssDNA or hpDNA) concentration. This analysis shows that RecBCD:hpDNA and RecBCD:ssDNA bind with 1:1 and 1:2 stoichiometric ratio. Previously, the stoichiometry binding of fluorescently labeled single stranded overhang (similar to substrate in Fig. 1C) had similar stoichiometry ratio to RecBCD heterotrimer [22].

Further analysis by analytic size exclusion chromatography (SEC) of RecBCD·hpDNA complex in comparison to RecBCD (Fig. 2B) shows clearly a monodisperse peak of approximate MW of ~330 kDa (determined by the linear range of known MW protein marker) in complex with the major peak of the hpDNA with a ratio of 1:1, 280:260 nm absorbance (in comparison to only RecBCD of 3:1, 280:260 ratio). This further confirms the stoichiometry of RecBCD: hpDNA of 1:1.

**DNA binding affinities to RecBCD and RecBCD·nucleotide complexes**

We analyzed different DNA substrates binding to RecBCD and RecBCD·nucleotide complexes by FA (Fig. 3A-E). All DNA binding isotherms exhibited hyperbolic dependence curves which enabled us to determine the equilibrium binding constants for the different DNA substrates (Table 2). Our binding model for the DNA substrates to RecBCD is described by the following stoichiometric reaction scheme (Scheme 1):

$$\text{RecBCD} + hp\text{DNA}/doh\text{DNA}/oh\text{DNA} \overset{K_D}{\rightleftharpoons} \text{RecBCD} \bullet x\text{DNA} \quad \text{(Scheme 1)}$$

Then the general solution for this equilibrium binding scheme is in the form of the following quadratic Equation 2:

$$[RecBCD \cdot DNA] = \frac{([RecBCD]_T + [DNA]_T + K_D) + \sqrt{([RecBCD]_T + [DNA]_T + K_D)^2 - 4[RecBCD]_T \cdot [DNA]_T}}{2} \quad \text{(Eq. 2)}$$

Where, $[DNA]_T$ is the monitored species; $[RecBCD]_T$ is titrated species and [RecBCD · DNA] is the bound species. For FA measurements, the condition to hold is that the total fluorescence intensity remains constant [23, 24] throughout the titration, and under our measurement conditions the changes in the FTI was small enough to be neglected, therefore allowing direct fitting of the FA binding isotherm curve using Eq. 2 to determine the equilibrium binding constants.

Initial binding of hpDNA to RecBCD in the absence and presence of nucleotide cofactors already revealed modulation in the affinities where ADP induced somewhat (3-fold) weaker affinity in comparison the APO state. In contrast, nucleotide cofactors did not show any dramatic effect on the affinity of RecBCD towards ssDNA binding.

When we tested the binding of dohDNA (Table 1C) to RecBCD·ADP (Fig. 3C, Table 2), we observed a dramatic change in the affinity, suggesting strong coupling between the binding sites. In the presence of ADP, RecBCD exhibited the strongest reduction in the affinity towards dohDNA substrates (40-fold and 25-fold, in comparison to APO and AMPpNp states, respectively, Table 2). This strong coupling between ADP and dohDNA binding may be key to reveal modulation in the affinity of RecBCD towards DNA to allow strong and weak binding states during ATPase cycling [25, 26]. To further dissect the source of the weak binding in the presence of ADP, we characterized the binding of two additional DNA substrates each containing either a 5ohDNA or 3ohDNA supposingly engaging with RecD or RecB, respectively (Fig. 1, Table 1). For both single stranded overhang substrates in the presence of ADP, RecBCD exhibits the strongest affinity in comparison when AMPpNp is bound or in the absence of a nucleotide cofactor (Fig. 3D &3 E).

Nonetheless, the strong coupling observed when both ssDNA overhangs 5' and 3' are engaged with RecB and RecD in the presence of ADP argues in favor of the existence of binding linkage. In contrast, when RecB or RecD are DNA free, the nucleotide state exhibited much weaker coupling among the three states, APO, AMPpNp or ADP bound. This suggests that there is some allosteric communication between RecB and RecD under the premise that both subunits are engaged with ssDNA via an element that may be outside the DNA binding sites within RecB and RecD. One explanation maybe that a full contact encompassing, RecB-Arm, RecB and RecD accounts for the observed strong coupling in the dohDNA.

**Analysis of ssDNA binding to RecBCD with the Hill Equation reveal cooperativity in the presence of ADP**

RecBCD binds two ssDNA, therefore we can utilize a binding model such as Hill to account for multiple binding sites according to Scheme 2:

$$\text{RecBCD} + ss\text{DNA} \xrightleftharpoons{K_D} \text{RecBCD} \bullet \left(ss\text{DNA}\right)_2 \qquad \text{(Scheme 2)}$$

to extract the two parameters $K_H$ and $n_H$ as shown in Equation 3:

$$\theta = \frac{[RecBCD]^n}{[RecBCD]^n + K^n} \qquad \text{(Eq. 3)}$$

Where, is θ the fraction bound $K$ is the apparent dissociation constant, $n$ is the Hill coefficient, while assuming that the ssDNA binding sites are similar, but not identical. The results obtained with fitting the data to the Hill equation provide further insights into the coupling between nucleotides and ssDNA binding. While the trend of the order of affinities towards ssDNA remains the same as with Eq. 2, the Hill coefficient in this case shows that while ADP weakens the affinity towards ssDNA, the cooperativity $n_H$ is increased to ~ 2. ssDNA binding to RecBCD has intermediate cooperativity whereas the presence of AMPpNp the cooperativity is slightly negative ($n_H$ ~ 0.7). This is a very exciting result as this suggests that when the two DNA

binding sites in RecB and RecD are bound with ssDNA, nucleotides cofactor impose different degree of cooperativity. Moreover, this was not revealed using the simple binding model.

**Nucleotides binding to RecBCD in the presence of DNA substrates exhibit biphasic binding patterns**

We have utilized FRET to measure the binding equilibrium constant for mant-Nucleotides derivatives to RecBCD (Zananiri, Gaydar, *et al.* 2017). Unique to RecBCD, the binding isotherm curves of mant-Nucleotides to RecBCD and RecBCD·DNA complexes all exhibited a biphasic binding pattern. Such binding is best described by the sum of two Hill plot (Zananiri, Gaydar, *et al.* 2017). Thus, mant-Nucleotide binding curves of the fluorescence change as a function of the free ligand concentration are best fitted to Equation 4:

$$y = p \cdot \frac{1}{1 + \left(\frac{K_s}{[mN]}\right)^{n_s}} + (1 - p) \cdot \frac{1}{1 + \left(\frac{K_w}{[mN]}\right)^{n_w}} \qquad \text{(Eq. 4)}$$

Where y is, the fraction bound, *mN* is the ligand concentration, $K_s$ (strong nucleotide state) and $K_w$ are the equilibrium constants of the first and second phase, respectively. $n_s$ and $n_w$ are the Hill coefficients of the first and second phase, respectively, and $p$ is the proportionality constant ($0 \leq p \leq 1$). Previously, we showed that the first phase of the binding titration curve reflects binding to the canonical ATP binding sites residing within RecB and RecD and the second phase describes binding to additional weak binding sites, both are given by macroscopic equilibrium constant's $K_s$ and $K_w$ (Zananiri, Gaydar, *et al.* 2017).

RecBCD and RecBCD·DNA complexes show overall $K_s$ values, ranging from ~13 to 140 μM and $n_s$ 0.8 to 3.0 (Table 3). The second binding phase exhibited $K_w$ values in the range of ~140 to 420 μM, an order of magnitude larger than $K_s$, indicating significantly weaker nucleotides' binding affinity sites (Table 3). In addition, those sites exhibit a degree of cooperativity, $n_w$, ranging from 2.5 to 12.0, but mostly with significant errors, indicating that

there may be some cooperative binding (Table 3) according to the Hill coefficient. However, we previously determined that there are at least two additional nucleotide binding sites in RecBCD and the high values of $n_w$ may be a result of an overestimation due to the resolution of the fit to accurately separate the two phases.

Overall there were four states that show strong modulation in the affinity parameter $\boldsymbol{K_s}$ as a result of the specific DNA substrates bound to RecBCD of the nucleotides state (Table 3). dohDNA bound to RecBCD induced a 2-fold weaker affinity of RecBCD towards AMPpNp in comparison to only RecBCD, and nearly no change in AMPpNp affinity towards RecBCD in complex with 5ohDNA and 3ohDNA (Figure 4A-D, Table 3). This suggests that the coupling between AMPpNp binding to RecBCD is apparent only when both ssDNA overhangs are present to fully interact with RecBCD. The presence of 3ohDNA only slightly weakens the affinity of RecBCD towards AMPpNp. Significantly, a much stronger effect of nucleotide binding affinity of RecBCD is amplified in the presence of dohDNA, specifically, in the ADP states. In this case, the affinity of RecBCD towards ADP is decreased ~7-fold in the presence of dohDNA towards ADP than in the absence of any other DNA substrates (Figure 4A-D, Table 3). Similarly, 5ohDNA and 3ohDNA weaken the affinity of RecBCD towards ADP with 7-fold and ~8-fold, respectively.

The affinity parameter $\boldsymbol{K_w}$ across all DNA substrates states appears to be changing very little in comparison to the ligated states of RecBCD without any DNA substrates (Table 3). This suggests that the weaker nucleotide binding sites (auxiliary sites) are much less prone to be affected by DNA binding. Overall, our results demonstrate that even though RecBCD cycles through an entire ATP hydrolysis states in less than a msec, still, nucleotide induced weak to strong transition and vice versa exists.

**RecBCD thermodynamic coupling between the nucleotide and DNA states**

Thermodynamic detailed balance analysis allows us to quantify the degree of linkage and the thermodynamic coupling constant (TC) between the DNA and nucleotide binding states. Figure 5 presents the five by two squares per each DNA substrate with two nucleotide binding states, AMPpNp and ADP. The ratio of binding affinities of a nucleotide in the presence or absence of DNA and vice versa, sheds a light on the mechanism by which RecBCD can switch from strong and weak binding states during processive translocation. The results of TC analysis for the cycles of hpDNA, ssDNA, dohDNA, 5ohDNA, and 3ohDNA in the absence or presence of either AMPpNp or ADP are summarized in Table 4.

Thermodynamic coupling constants across the thermodynamics detailed balance square should be equal, i.e., $K_{Mp,hp}/K_{Mp} \cong K_{hp,Mp}/K_{hp}$, due to consideration of the total free energy change within a closed cycle. Thus, near equalities of TC provide an intrinsic measure of the consistency within each ligated state. Inspection of the TC in Table 4, reveals that this criterion is met to the accuracy of the measurements in most of the cycles. However, in the case of $(K_{D,doh}/K_D)/(K_{doh,D}/K_{doh})$, $(K_{D,5oh}/K_D)/(K_{5oh,D}/K_{5oh})$ and $(K_{D,3oh}/K_D)/(K_{3oh,D}/K_{3oh})$, the ratio between the TC pairs are, ~0.13, ~18, and ~30, respectively. The simplest explanation for this deviation in the TC equality could be the results of the binding model i.e., DNA or nucleotide binding isotherms are not accurately reflecting the macroscopic equilibrium constants in s these cases. This is due to the nature of the multiple binding sites of both DNA and nucleotide binding. The other is that the assumption under which equilibrium balance holds, i.e., the equilibrium is invariant under the time frame does not hold and these complexes are slowly interchanging even under steady state measurements with these DNA substrates. Currently, we cannot differentiate between these possibilities or what is the source of this imbalance. However, further

measurements under higher stabilizing conditions may be important to resolve these differences. In summary, we show using TC that distinct states are induced to disturb the TC ratio to a degree where strong and weak coupling are observed between the strong nucleotides binding sites in the presence of dohDNA substrate with a much higher degree in ADP state.

**Discussion**

In this work, we have investigated the nucleotide binding linkage of RecBCD to determine quantitatively the degree of coupling between the different nucleotide states with the different DNA substrates. Our results suggest that RecBCD TC is a highly complex network partly due to the number of DNA contact sites within the different protomers, the two catalytic ATP sites and furthermore, the long range weak effect of the auxiliary nucleotide sites. We find that in order to induce linkage between DNA and nucleotide binding, the DNA substrates, such as dohDNA, must be fully engage with both translocase activities and with the RecB ARM. The ADP states seem to induce the strongest coupling in comparison to the APO or AMPpNp bound states. In this regard, all three substrates, dohDNA, 5ohDNA and 3ohDNA are affecting ADP binding unlike AMPpNp. When RecBCD is bound to ADP, the strongest effect is observed in the binding towards dohDNA affinity while the 5ohDNA and 3ohDNA are much less affected in comparison to the APO states. This asymmetry between the reciprocal effects that the latter two substrates have on ADP binding to RecBCD could simply be due to measuring one experiment with end labeled 5' DNA versus unlabeled DNA in the latter experiments. However, this would only affect the magnitude of their mutual effect on binding, but not the actual observed strong coupling. Therefore, we conclude that the ADP binding state is key to promote weak binding towards DNA, mostly when dohDNA is utilized but also when 5ohDNA and 3ohDNA. If ADP induces in both subunits RecB and RecD weak binding towards DNA, it will require that these

states will never coexist in both subunits at the same time to the same extent. Furthermore, the additional parameter for the synchronized DNA binding mechanism by the two helicase subunits of RecBCD, could be reflected in a Hill coefficient >1 (Table 3). This is apparent in the case of ssDNA binding or in the nucleotide binding in the presence of DNA substrates that are engaged by multiple subunits simultaneously (Table 4, ssDNA, dohDNA, 3ohDNA and 5ohDNA).

One exception exists for 3ohDNA substrate which exhibits overall weaker affinity in the absence or presence of AMPpNp in comparison to when ADP is bound. However, the TC for these states, $K_{Mp,3oh}/K_{Mp}$ and $K_{3oh,Mp}/K_{3oh}$ is very weakly coupled and the detailed balance are consistent with the thermodynamic cycle among these states suggesting that, although there may be wakening in the affinity among these states they don't trigger the strong coupling affects as observed with ADP in the presence of dohDNA.

Structural investigation of RecBCD provided wealth of information in regards to the DNA contact sites within RecBCD subunits, however still missing are structures with different nucleotide states to reveal the conformational changes induced by the different ligated states. Nonetheless, inspection of the RecBCD structure clearly shows the large surface area that makes direct contacts with the DNA [5]. At the forefront, the RecB ARM makes extensive contacts with the dsDNA. This is followed by more contacts of the C-terminal and the junction of the dsDNA with the 'pin' domain of RecC. RecB 2A subdomain interacts with the 3' overhang ssDNA, while RecD subdomain 1A and 2A make contacts with the 5' overhang ssDNA [5]. Correlating the coupling between DNA and nucleotide binding is crucial to elucidate the mechanism of RecBCD successive translocation. Strong binding states can be viewed as the 'pulling' states while the weak binding states are the 'relieving' states allowing for productive advancement of RecBCD motor while alternating these events between RecB and RecD.

Therefore, allosteric communication will most likely exist and will involve network of interactions across all the DNA contact sites throughout all RecBCD subunits.

Thus, driven by our present work, we suggest that RecBCD has enzymatically evolved to go through these essential biochemical intermediates with minimum 'effort', with minimum energy barriers but still maintain their existence within any mechanism to allow translocation. Weather the alteration between strong and weak binding states of RecBCD is synchronized among its subunits by the nucleotide state during its processive unwinding is probably prerequisite to allow high efficiency of ATP utilization. Therefore, it will be most interesting to study how such mechanism is enabled within RecBCD ATPase subunits.

Although we have not accessed all possible states, our analysis of the APO state, ATP mimicking state and the ADP state after P*i* release, with hpDNA, ssDNA, dohDNA, 5ohDNA, and 3ohDNA represent a wide array of biochemical intermediates along the reaction coordinates of RecBCD.

**Funding**

This research was supported by The Israel Science Foundation [grant No. 296/13]; and the Marie Curie Career Integration Award [grant No. 1403705/11].

**Acknowledgments**

We thank Dr. Stephen C. Kowalczykowski and Dr. Theetha Pavankumar for the RecBCD expression system and their assistance in RecBCD purification protocol (University of California, Davis, California). We thank Boris Shneyer for critically reading the manuscript.

## Materials and Methods

### Reagents and Purification of RecBCD

All chemicals and reagents were the highest purity commercially available. ATP and ADP were purchased from Roche Molecular Biochemicals (Indianapolis, IN, USA). Adenosine 5′-(β,γ-imido)triphosphate (AMPpNp) was purchased from Sigma (St. Louis, MO, USA). A molar equivalent of $MgCl_2$ was added to nucleotides immediately before use. Nucleotide concentrations were determined by absorbance using an extinction coefficient $\varepsilon_{259}$ of 15,400 $M^{-1}$ $cm^{-1}$. The concentrations of N-methylanthraniloyl (mant) derivatives of ADP, 2'-deoxyADP, ATP, and 2'-deoxyATP (Jena Bioscience, Jena, Germany) were determined using $\varepsilon_{255}$ of 23,300 $M^{-1}$ $cm^{-1}$. Unless otherwise specified, all experiments were conducted in RecBCD Buffer (RB: 20 mM MOPS pH 7.4, 2 mM MgCl2, 1 mM DTT, 0.1 mM EDTA and, unless specified, 75 NaCl. Over-expression and purification of recombinant RecBCD was based on the method described by Roman et. al.[27], with additional step as indicated. All steps of purification were carried out at 4 °C, and contained 20 mM MOPS pH 7.4, 2 mM $MgCl_2$,1 mM DTT, 0.1 mM EDTA, 1 mM PMSF, 1 mM Benzamidine and the indicated salt concentration. Four liters of *E.coli* cells expressing RecBCD were lysed using Microfluidizer, followed by centrifugation at 10,000×g. The supernatant was further clarified by centrifugation at 100,000×g and treated with Benzonase for two hrs before initial purification by DEAE chromatography (weak anion exchanger to remove nucleic acids contaminants) using a linear NaCl gradient from 75 mM to 700 mM. RecBCD-containing DEAE fractions were eluted from a Q-sepharose column (strong anion exchanger which highly selects for active RecBCD [28] using a linear NaCl gradient from 75 mM to 1 M. Fractions containing RecBCD were precipitated using $(NH_4)_2SO_4$ (45% saturation), and collected by centrifugation at 14,000×g. Precipitated RecBCD was resuspended

and loaded onto Superdex 200 equilibrated with RB , as a final step of polishing and elution of RecBCD specifically from the monodisperse peak of the heterotrimer complex of RecBCD. Fractions containing purified RecBCD were concentrated using an Amicon concentrator (50 kDa cutoff), aliquoted and flash frozen in liquid nitrogen before storage at -80°C. The RecBCD concentration was determined using $\varepsilon_{ex,coeff.}$ of $4.2\times10^5$ $M^{-1}$ $cm^{-1}$ in Guanidine chloride. To ensure RecBCD purity from nucleic acids, only protein fractions with 280/260 nm ratio >1.3 were used (Zananiri, Gaydar, *et al.* 2017).

**DNA substrates:**

DNA oligonucleotides were purchased from IDT (Leuven, Belgium) and HPLC purified. The DNA substrates shown in Figure 2 were obtained by folding or hybridization of the DNA in 20 mM MOPS pH 7.4, 75 mM NaCl, 1 mM $MgCl_2$ buffer at 85°C for 3 minutes followed by slow cooling to room temperature before storage at -20°C.

**DNA binding measurements by Fluorescence Anisotropy (FA):**

FA measurements were performed with a PC1 spectrofluorimeter set up T-format configuration for simultaneous acquisition on two emission channels using monochromators equipped with automatic polarizers. Samples were equilibrated (60 min, RT) and then measured with $\lambda_{ex}$ = 492 nm using vertical polarized light and the emitted vertical and horizontal polarized light was monitored at 90° with emission monochromators at $\lambda_{em}$ =523 nm at 25 ± 0.1°C. G-factor for correction of the different gain between of vertical and horizontal PMT detectors was calculated as described by the instrument manufacturer. The buffer included 20 mM MOPS pH 7.4, 2 mM $MgCl_2$, 1 mM DTT, and 75 mM NaCl. Nucleotides concentrations in the measurements where indicated were 2 mM (MgADP, or MgAMPpNp). Fluorescent DNA substrates were held constant at 25 nM.

**mant-Nucleotide binding to RecBCD by Förster resonance energy transfer (FRET):**

FRET measurements were performed with a PC1 spectrofluorimeter (ISS, Champaign, IL), utilizing excitation and emission monochromators. The observation cell was regulated with Peltier temperature controller at 25 ± 0.1°C. All equilibrium binding reactions were performed in a 10 µl Precision cell fluorescence cuvette (Farmingdale, NY, USA), which allows minimal inner filter affects [29] up to concentration of ~ 550 µM mantNucleotides. The buffer included 20 mM MOPS pH 7.4, 2 mM $MgCl_2$, 1 mM DTT, and varying concentrations of NaCl (75, 150, 200, 300 mM). mant-nucleotides were titrated with 1:1 ratio to $MgCl_2$. Equilibrium binding reactions of mantNucleotides to RecBCD were measured by FRET between RecBCD intrinsic tryptophan fluorescence ($\lambda_{ex}$ = 280 nm) and bound mantNucleotide (fluorescence monitored at 90° through an emission monochromoter at $\lambda_{em}$ = 436 nm) [30]. We performed subtractions of background fluorescence of free nucleotides on the observed emission peak. DNA substrates were held constant at 1 µM and RecBCD concertation was 1 µM. In the case of ADP binding to RecBCD·dohDNA, the DNA concentration was 8 µM.

## References

[1] Smith GR. How RecBCD enzyme and Chi promote DNA break repair and recombination: a molecular biologist's view. Microbiology and molecular biology reviews : MMBR. 2012;76:217-28.
[2] Liu B, Baskin RJ, Kowalczykowski SC. DNA unwinding heterogeneity by RecBCD results from static molecules able to equilibrate. Nature. 2013;500:482-5.
[3] Boehmer PE, Emmerson PT. The RecB subunit of the Escherichia coli RecBCD enzyme couples ATP hydrolysis to DNA unwinding. The Journal of biological chemistry. 1992;267:4981-7.
[4] Dillingham MS, Spies M, Kowalczykowski SC. RecBCD enzyme is a bipolar DNA helicase. 2003;423.
[5] Singleton MR, Dillingham MS, Gaudier M, Kowalczykowski SC, Wigley DB. Crystal structure of RecBCD enzyme reveals a machine for processing DNA breaks. Nature. 2004;432:187-93.
[6] Masterson C, Boehmer PE, McDonald F, Chaudhuri S, Hickson ID, Emmerson PT. Reconstitution of the activities of the RecBCD holoenzyme of Escherichia coli from the purified subunits. The Journal of biological chemistry. 1992;267:13564-72.
[7] Taylor AF, Smith GR. Monomeric RecBCD Enzyme Binds and Unwinds DNA. Journal of Biological Chemistry. 1995;270:24451-8.
[8] Taylor AAF, Smith GRG. RecBCD enzyme is a DNA helicase with fast and slow motors of opposite polarity. Nature. 2003;423:889-93.
[9] Spies M, Amitani I, Baskin RJ, Kowalczykowski SC. RecBCD enzyme switches lead motor subunits in response to chi recognition. Cell. 2007;131:694-705.
[10] Xie F, Wu CG, Weiland E, Lohman TM. Asymmetric regulation of bipolar single-stranded DNA translocation by the two motors within Escherichia coli RecBCD helicase. The Journal of biological chemistry. 2013;288:1055-64.
[11] Wong I, Lohman TM. Allosteric effects of nucleotide cofactors on Escherichia coli Rep helicase-DNA binding. Science. 1992;256:350-5.
[12] Patel SS, Donmez I. Mechanisms of helicases. J Biol Chem. 2006;281:18265-8.
[13] Lohman TM, Tomko EJ, Wu CG. Non-hexameric DNA helicases and translocases: mechanisms and regulation. Nat Rev Mol Cell Biol. 2008;9:391-401.
[14] Olivares AO, De La Cruz EM. Holding the reins on myosin V. Proc Natl Acad Sci U S A. 2005;102:13719-20.
[15] von Hippel PH. Helicases become mechanistically simpler and functionally more complex. Nat Struct Mol Biol. 2004;11:494-6.
[16] Hackney DD. The kinetic cycles of myosin, kinesin, and dynein. Annu Rev Physiol. 1996;58:731-50.
[17] Lohman TM, Thorn K, Vale RD. Staying on track: common features of DNA helicases and microtubule motors. Cell. 1998;93:9-12.
[18] Henn A, Bradley MJ, De La Cruz EM. ATP utilization and RNA conformational rearrangement by DEAD-box proteins. Annu Rev Biophys. 2012;41:247-67.
[19] Henn A, Sadot E. The unique enzymatic and mechanistic properties of plant myosins. Curr Opin Plant Biol. 2014;22C:65-70.
[20] Batters C, Veigel C. Mechanics and Activation of Unconventional Myosins. Traffic. 2016;17:860-71.

[21] Wong CJ, Lohman TM. Kinetic control of Mg2+-dependent melting of duplex DNA ends by Escherichia coli RecBC. Journal of molecular biology. 2008;378:761-77.
[22] Wu CG, Bradford C, Lohman TM. Escherichia coli RecBC helicase has two translocase activities controlled by a single ATPase motor. Nature structural & molecular biology. 2010;17:1210-7.
[23] Otto MR, Lillo MP, Beechem JM. Resolution of multiphasic reactions by the combination of fluorescence total-intensity and anisotropy stopped-flow kinetic experiments. Biophys J. 1994;67:2511-21.
[24] Henn A, Cao W, Licciardello N, Heitkamp SE, Hackney DD, De La Cruz EM. Pathway of ATP utilization and duplex rRNA unwinding by the DEAD-box helicase, DbpA. P Natl Acad Sci USA. 2010;107:4046-50.
[25] Saikrishnan K, Griffiths SP, Cook N, Court R, Wigley DB. DNA binding to RecD: role of the 1B domain in SF1B helicase activity. EMBO J. 2008;27:2222-9.
[26] Wong CJ, Lucius AL, Lohman TM. Energetics of DNA end binding by E.coli RecBC and RecBCD helicases indicate loop formation in the 3'-single-stranded DNA tail. Journal of molecular biology. 2005;352:765-82.
[27] Roman LJ, Kowalczykowski SC. Characterization of the helicase activity of the Escherichia coli RecBCD enzyme using a novel helicase assay. Biochemistry. 1989;28:2863-73.
[28] Bianco PR, Kowalczykowski SC. The recombination hotspot Chi is recognized by the translocating RecBCD enzyme as the single strand of DNA containing the sequence 5'-GCTGGTGG-3'. Proc Natl Acad Sci U S A. 1997;94:6706-11.
[29] Birdsall B, King RW, Wheeler MR, Lewis CA, Jr., Goode SR, Dunlap RB, et al. Correction for light absorption in fluorescence studies of protein-ligand interactions. Anal Biochem. 1983;132:353-61.
[30] Talavera MA, De La Cruz EM. Equilibrium and kinetic analysis of nucleotide binding to the DEAD-box RNA helicase DbpA. Biochemistry. 2005;44:959-70.

## Figure Legends

**Figure 1**: **Schematic representation of the DNA substrates used in this work**. **A.** Hairpin DNA: hpDNA, hpDNA-F (Table 1, 1a, b) **B.** Single strand DNA: ssDNA, ssDNA-F (Table 1, 2a, b), **C.** Double strand overhang DNA: dohDNA, dohDNA-F (Table 1, 3a, b), **D.** Single strand overhang DNA: 5ohDNA, 5ohDNA-F (Table 1, 4a, b), **E.** Single strand overhang DNA: 3ohDNA, 3ohDNA-F (Table 1, 5a, b); FAM: 6-fluorescein amidi.

**Figure 2: Purification and Biochemical characterization of RecBCD oligomeric states without and with DNA and nucleotides. A.** Stoichiometric titration of RecBCD versus ssDNA and hpDNA using FA. Concentration of ssDNA/hpDNA were fixed at 2 μM, and RecBCD was titrated up to 10 μM (5-fold DNA concentration). The fitted curve shown in black line is according to Eq. 1. This produced the following "n" values for RecBCD/ssDNA = 0.49 ± 0.1 and RecBCD/hpDNA = 1.12 ± 0.1. Data shown as mean ± s.e.m., n=2. **B.** Analytical SEC analysis by Superdex 200 of RecBCD oligomeric state in the absence and presence of hpDNA under stoichiometric conditions. The absorption spectra was normalized for its presentation. RecBCD absorption ratio 280 nm:260 nm for RecBCD in the absence of hpDNA is 3:1, in the presence hpDNA the ratio is 1:1, therefore enable the determination of hpDNA presence in RecBCD peak. Peak of RecBCD·hpDNA, corresponding to a molecular weight of ~ 330 kDa according to the MW standards.

**Figure 3: Fluorescence Anisotropy equilibrium binding measurements of RecBCD and RecBCD·nucleotides complex to fluorescently labeled DNA.** DNA substrates were labaled with 6-fluorescein amidi. Fluroesecne DNA was held at 25 nM and RecBCD was titrated to obtain saturation of the binding isotherm. The specifc DNA in each figure is labelled in accordance to RecBCD (●), RecBCD·AMPpNp (●) RecBCD·ADP (●), **A.** F-hpDNA binding

isotherms, **B.** F-ssDNA binding isotherms, **C.** F-dohDNA binding to binding isotherms, **D**. F-5ohDNA binding isotherms, **E.** F-3ohDNA binding isotherms, Solid lines through the data points (A-E) are the best fit to Eq.2. **F.** Data in B fitted to a Hill equation model. Error bars report the s.d of three independent measurements, n = 3. $\lambda_{ex}$ = 492 nm and $\lambda_{em}$ = 523 nm. Nucleotides concentrations where indicated were 2 mM (MgADP, or MgAMPpNp).

**Figure 4: Equilibrium binding of RecBCD and RecBCD·DNA to mantNucleotides.** **A. and B.** Titration curves of mantAMPpNp (A) and mantADP (B) binding to RecBCD and RecBCD·DNA substrates exhibit biphasic pattern. Data points are normalized as fraction bound. (A) and (B) RecBCD (●), RecBCD·hpDNA (●), RecBCD·ssDNA (●), **C. and D.** titration curves of mantAMPpNp (C) and mantADP (D) binding to RecBCD and RecBCD·DNA substrates exhibit biphasic pattern. RecBCD·dohDNA (●), RecBCD·5ohDNA (●), and RecBCD·3ohDNA (●). Lines show the best fit to Eq. 3. Data shown as mean ± s.e.m., n = 3.

**Figure 5: Detailed thermodynamic balance schemes of RecBCD ligated states.** The schemes describe the ligated states of the initiation complex (first row, hairpin DNA, stoichiometry 1:1), translocation complex (second row, ssDNA, stoichiometry 1:2), unwinding complex (third row, dohDNA, stoichiometry 1:1). The boxes in the fourth and fifth rows are asymmetric substrates engaged either with RecD (5ohDNA) or RecB (3ohDNA) only. The equilibrium constants, and hence the nucleotide binding occupancy in the model are relating only to the strong nucleotide binding sites. The equilibrium constants and the free energy calculated are shown in Tables 2 and 3 and are according to the detailed balanced shown in the reaction schemes. H - RecBCD, hp - hpDNA, ss - ssDNA, doh - dohDNA, 5oh - 5ohDNA, 3oh - 3ohDNA, D - ADP, Mp -

AMPpNp, RecBCD enzyme is represented by orange, green, blue ovals for RecB, RecC and RecD, respectively. DNA is drawn as black solid lines.

**Tables**

**Table 1: Sequences of the DNA substrates used for DNA and nucleotides binding experiments**

| # | Sequence Description | Sequence 5' - 3' | DNA Length |
|---|---|---|---|
| 1a | 21 bp hairpin DNA | CATGTGACTCGTTACCTGAGTTTTTACTCAGGTAACGAGTCACATG | 46 |
| 1b | 21 bp hairpin DNA 3' FAM | GATGTGACTCGTTACCTGAGTTTTTACTCAGGTAACGAGTCACATC-FAM | 46 |
| 2a | 24 nt ssDNA | AGAGAGAGAGAGAGAGAGAGAGAG | 24 |
| 2b | 24 nt ssDNA 5' FAM | FAM-AGAGAGAGAGAGAGAGAGAGAGAG | 24 |
| 3a | 10-6 nt 5'-3' overhang | CGCGCGCATGTGACTCGTTACCTGAGTTTTTACTCAGGTAACGAGTCACATGATATATATATAT | 62 |
| 3b | 10-6 nt 5'-3' overhang FAM | FAM-CGCGCGCATGTGACTCGTTACCTGAGTTTTTACTCAGGTAACGAGTCACATGATATATATATAT | 62 |
| 4a | 6 nt 5' overhang | CGCGCGCATGTGACTCGTTACCTGAGTTTTTACTCAGGTAACGAGTCACATG | 52 |
| 4b | 6 nt 5' overhang FAM | FAM-CGCGCGCATGTGACTCGTTACCTGAGTTTTTACTCAGGTAACGAGTCACATG | 52 |
| 5a | 10 nt 3' overhang | CATGTGACTCGTTACCTGAGTTTTTACTCAGGTAACGAGTCACATGATATATATATAT | 56 |
| 5b | 10 nt 3' overhang FAM | FAM-CATGTGACTCGTTACCTGAGTTTTTACTCAGGTAACGAGTCACATGATATATATATAT | 56 |

1. FAM: 6-fluorescein amidi

**Table 2: Equilibrium constants for DNA substrates binding to RecBCD and RecBCD·nucleotides complex.**

| Annotation | Complex | [1]$K_D$ (nM) | | $\Delta G°'_{association}$ (kJ·mol$^{-1}$) |
|---|---|---|---|---|
| $K_{hp}$ | RecBCD·hpDNA-F | 42 ± 9 | | - 42.1 ± 0.5 |
| $K_{hp,Mp}$ | RecBCD·AMPpNp·hpDNA-F | 85 ± 19 | | - 40.3 ± 0.6 |
| $K_{hp,D}$ | RecBCD·ADP·hpDNA-F | 127 ± 31 | | - 39.3 ± 0.6 |
| $K_{ss}$ | RecBCD·ssDNA-F | 7 ± 2 | | - 46.6 ± 0.5 |
| $K_{ss,Mp}$ | RecBCD·AMPpNp·ssDNA-F | 4.5 ± 2 | | - 47.6 ± 1.8 |
| $K_{ss,D}$ | RecBCD·ADP·ssDNA-F | 13 ± 5 | | - 45.0 ± 0.2 |
| $K_{doh}$ | RecBCD·dohDNA-F | 19.2 ± 5 | | - 44.0 ± 0.6 |
| $K_{doh,Mp}$ | RecBCD·AMPpNp·dohDNA | 34.0 ± 7.0 | | - 42.6 ± 0.5 |
| $K_{doh,D}$ | RecBCD·ADP·dohDNA | 823.0 ± 261.0 | | - 34.7 ± 0.8 |
| $K_{5oh}$ | RecBCD·5ohDNA-F | 29.6 ± 7 | | - 43.0 ± 0.6 |
| $K_{5oh,Mp}$ | RecBCD·AMPpNp·5ohDNA-F | 31 ± 8 | | - 43.0 ± 0.6 |
| $K_{5oh,D}$ | RecBCD·ADP·5ohDNA-F | 8 ± 2 | | - 46.2 ± 0.6 |
| $K_{3oh}$ | RecBCD·3ohDNA-F | 92.6 ± 15.4 | | - 40.1 ± 0.4 |
| $K_{3oh,Mp}$ | RecBCD·AMPpNp·3ohDNA-F | 166.3 ± 41 | | - 38.7 ± 0.6 |
| $K_{3oh,D}$ | RecBCD·ADP·3ohDNA-F | 16.3 ± 7 | | - 44.4 ± 1.1 |
| | | **$K_H$ (nM)** | **$n_H$** | |
| $K_{ss}$ | RecBCD·ssDNA-F | 16.5 ± 3.1 | 1.4 ± 0.32 | - 44.4 ± 0.5 |
| $K_{ss,Mp}$ | RecBCD·AMPpNp·ssDNA-F | 7.0 ± 5.0 | 0.7 ± 0.20 | - 46.5 ± 1.8 |
| $K_{ss,D}$ | RecBCD·ADP·ssDNA-F | 23.1 ± 2.2 | 2.1 ± 0.34 | - 43.6 ± 0.2 |

[1]Equilibrium constants reflect the macroscopic binding affinity of DNA binding to RecBCD complex

**Table 3: Equilibrium constants for nucleotides binding to RecBCD and RecBCD·DNA complexes**

| Annotation | Complex | $K_s$(μM) | $n_s$ | $K_w$ (μM) | $n_w$ | $p$ | $\Delta G_s°'_s$ (kJ·mol$^{-1}$) | $\Delta G_w°'_s$ (kJ·mol$^{-1}$) |
|---|---|---|---|---|---|---|---|---|
| $^4K_{Mp}$ | RecBCD·mMp | 52.4 ± 7.8 | 0.99 ± 0.1 | 286.9 ± 11.9 | 12.0 ± 4.7 | 0.60 ± 0.04 | -24.4 ± 0.4 | -20.2 ± 0.1 |
| $K_{Mp,hp}$ | RecBCD·hpDNA·mMp | 73.5 ± 9.3 | 1.44 ± 0.3 | 147.0 ± 6.8 | 5.0 ± 1.1 | 0.74 ± 0.1 | -23.6 ± 0.3 | -21.9 ± 0.1 |
| $K_{Mp,ss}$ | RecBCD·ssDNA·mMp | 20.0 ± 5.9 | 2.90 ± 0.9 | 146.9 ± 6.8 | 5.0 ± 1.1 | 0.23 ± 0.1 | -26.8 ± 0.7 | -21.9 ± 0.1 |
| $K_{Mp,doh}$ | RecBCD·dohDNA·mMp | 106 ± 33.5 | 1.8 ± 0.4 | 343.8 ± 9.2 | 9.0 ± 3.2 | 0.50 ± 0.1 | -22.7 ± 0.8 | -19.6 ± 0.2 |
| $K_{Mp,5oh}$ | RecBCD·5ohDNA·mMp | 47.8± 22.1 | 2.0 ± 1.0 | 285.1 ± 17.9 | 4.1 ± 0.8 | 0.30 ± 0.1 | -24.6 ± 1.1 | -19.8 ± 0.1 |
| $K_{Mp,3oh}$ | RecBCD·3ohDNA·mMp | 71 ± 28.3 | 1.7 ± 0.4 | 295.8 ± 12.1 | 5.2 ± 1.5 | 0.50 ± 0.1 | -23.7 ± 1.0 | -20.2 ± 0.2 |
| $^4K_{mD}$ | RecBCD·mD | 13.2 ± 3.1 | 0.95 ± 0.1 | 322.5 ± 6.9 | 6.2 ± 0.6 | 0.45 ± 0.03 | -27.8 ± 0.6 | -20.1 ± 0.1 |
| $K_{D,hp}$ | RecBCD·hpDNA·mD | 29.2 ± 11.8 | 0.81 ± 0.2 | 314.9 ± 22.0 | 4.0 ± 0.3 | 0.51 ± 0.12 | -25.9 ± 1.0 | -20.0 ± 0.2 |
| $K_{mD,ss}$ | RecBCD·ssDNA·mD | 15.7 ± 3 | 2.85 ± 1.7 | 343.0 ± 84.2 | 2.5 ± 0.8 | 0.19 ± 0.01 | -27.4 ± 0.5 | -19.8 ± 0.6 |
| $K_{mD,doh}$ | RecBCD·dohDNA·mD | 70.9 ± 19.4 | 1.5 ± 0.3 | 338.3 ± 8.9 | 9.0 ± 3.0 | 0.51 ± 0.1 | -23.7 ± 0.7 | -19.8 ± 0.1 |
| $K_{mD,5oh}$ | RecBCD·5ohDNA·mD | 70.5 ± 8.6 | 2.4 ± 0.4 | 354.4 ± 17.7 | 5.3 ± 1.1 | 0.38 ± 0.1 | -23.7 ± 0.3 | -19.7 ± 0.1 |
| $K_{mD,3oh}$ | RecBCD·3ohDNA·mD | 80.8± 25.7 | 1.5 ± 0.3 | 342.2 ± 7.5 | 5.9 ± 1.2 | 0.44 ± 0.2 | -23.3 ± 0.8 | -19.8 ± 0.1 |

1. mantADP (mD); mantAMP-pNp (mMp);

2. Fitted parameters for the sum of two Hills equations, $\boldsymbol{K_s}$ & $\boldsymbol{K_w}$ are the equilibrium dissociation constants for nucleotides association to the strong and weak binding sites, respectively; $\boldsymbol{n_s}$ & $\boldsymbol{n_w}$ are the Hill coefficients for nucleotides' association to the strong and the weak binding sites, respectively.

3. $\Delta G°'_s = RTln(K_s)$ and $\Delta G°'_w = -RTln(K_{sw})$ are the standard binding energies at 1 M ligand, R is the gas constant (8.314 J mol$^{-1}$ $K^{-1}$), T = 298.15°K for the strong and weak binding sites, respectively.

4. Previously reported (Zananiri & Gaydar *et al.* 2017).

**Table 4. Thermodynamic coupling parameters associated with RecBCD, RecBCD·DNA, RecBCD·DNA· nucleotide complexes**

| Detailed thermodynamic square | Thermodynamic coupling parameter | [1]Thermodynamic coupling constant |
|---|---|---|
| *Mp,hp* | $K_{Mp,hp}/K_{Mp}$ | 1.4 |
| | $K_{hp,Mp}/K_{hp}$ | 2 |
| *D,hp* | $K_{D,hp}/K_{D}$ | 2.2 |
| | $K_{hp,D}/K_{hp}$ | 3 |
| *Mp,ss* | $K_{Mp,ss}/K_{Mp}$ | 0.4 |
| | $K_{ss,Mp}/K_{ss}$ | 0.6 |
| *D,ss* | $K_{D,ss}/K_{D}$ | 1.2 |
| | $K_{ss,D}/K_{ss}$ | 1.9 |
| *Mp,doh* | $K_{Mp,doh}/K_{Mp}$ | 2 |
| | $K_{doh,Mp}/K_{doh}$ | 1.8 |
| *D,doh* | $K_{D,doh}/K_{D}$ | 5.4 |
| | $K_{doh,D}/K_{doh}$ | 42.9 |
| *Mp,5oh* | $K_{Mp,5oh}/K_{Mp}$ | 0.9 |
| | $K_{5oh,Mp}/K_{5oh}$ | 1 |
| *D,5oh* | $K_{D,5oh}/K_{D}$ | 5.3 |
| | $K_{5oh,D}/K_{5oh}$ | 0.3 |
| *Mp,3oh* | $K_{Mp,3oh}/K_{Mp}$ | 1.4 |
| | $K_{3oh,Mp}/K_{3oh}$ | 1.8 |
| *D,3oh* | $K_{D,3oh}/K_{D}$ | 6.1 |
| | $K_{3oh,D}/K_{3oh}$ | 0.2 |

1. Calculated from detailed thermodynamic squares Fig. 5.

**Figure 1**

| A. | | B. | | C. | | D. | | E. | |
|---|---|---|---|---|---|---|---|---|---|
| hpDNA | hpDNA-F | ssDNA | ssDNA-F | dohDNA | dohDNA-F | 5ohDNA | 5ohDNA-F | 3ohDNA | 3ohDNA-F |

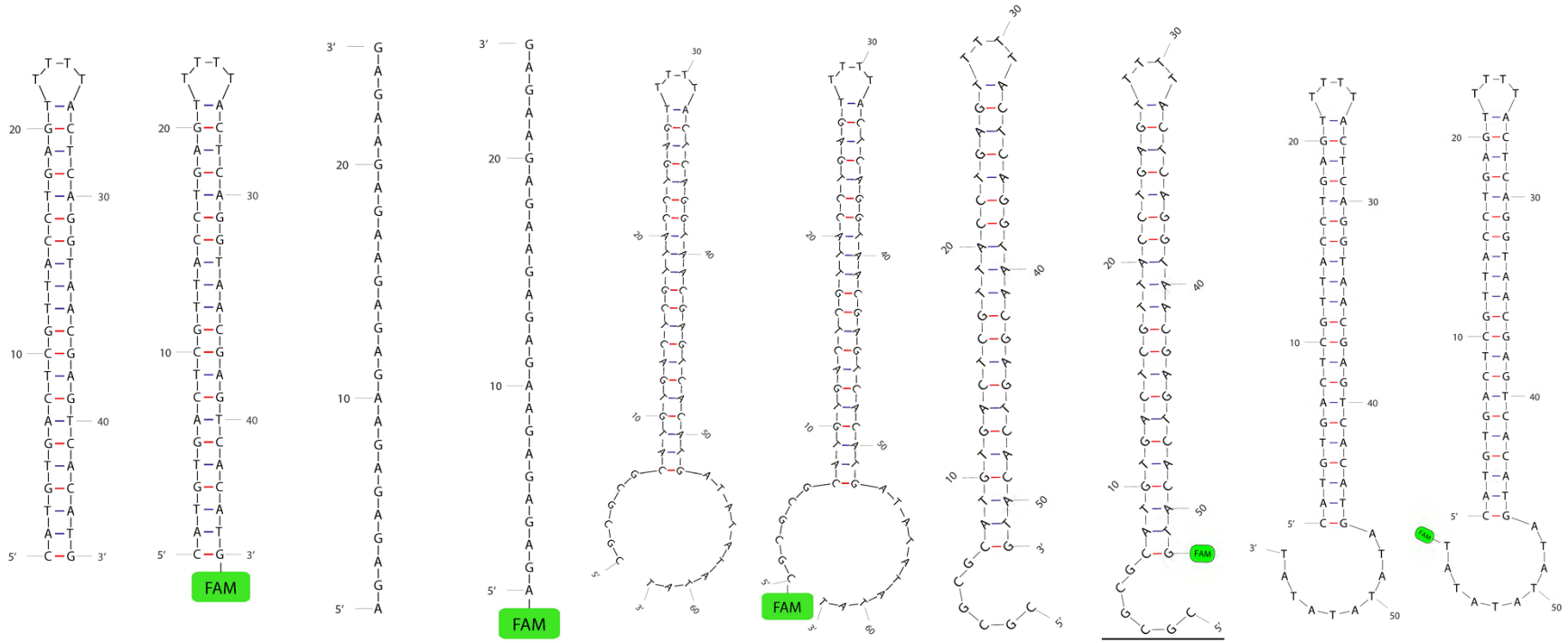

**Figure 2**

**A.**

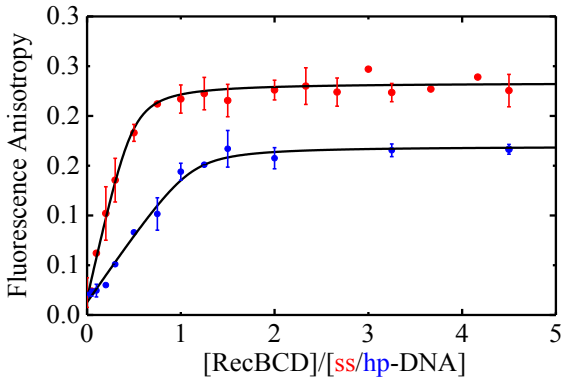


**B.**

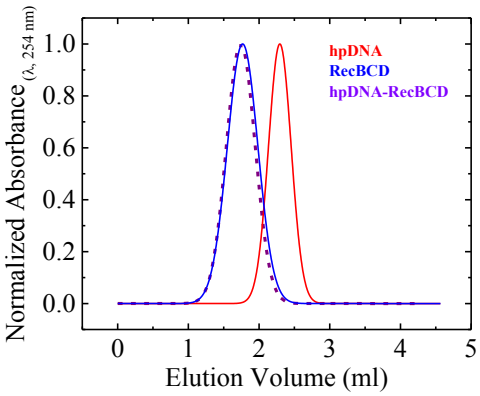

**Figure 3**

**A.**

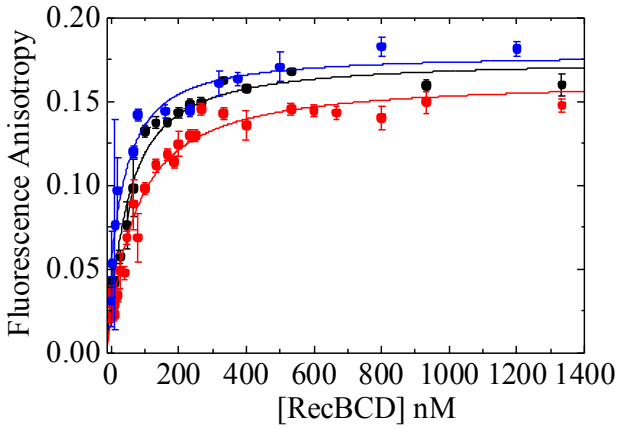


**B.**

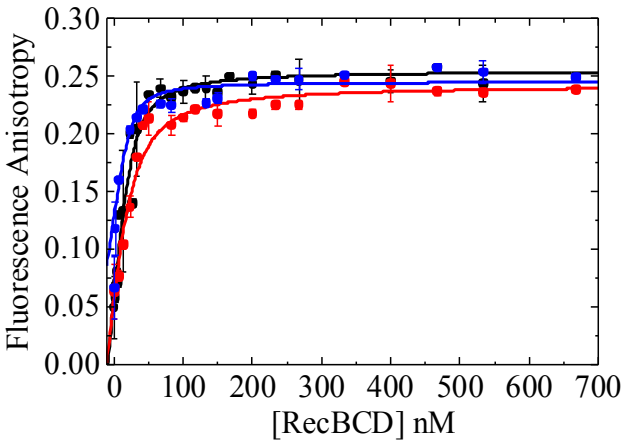


**C.**

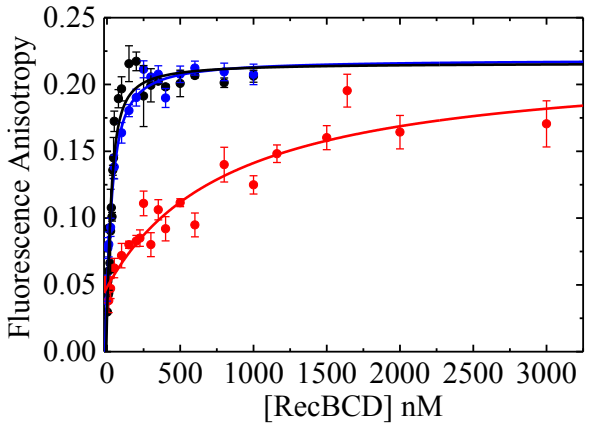


**D.**

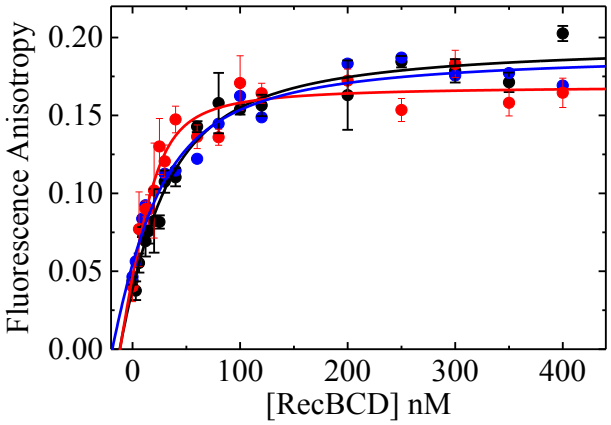


**E.**

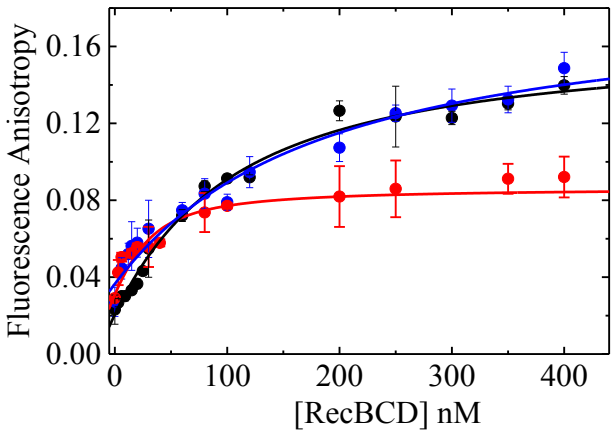


**F.**

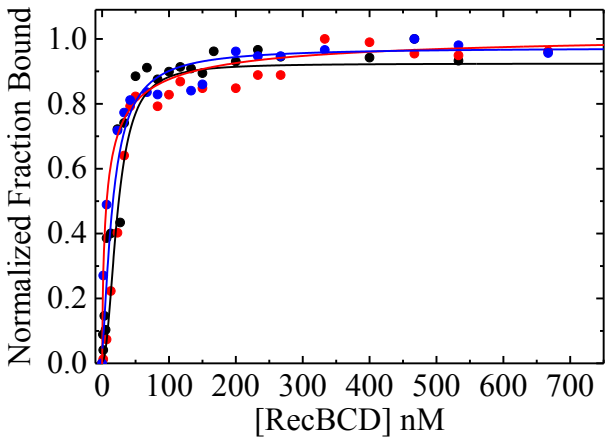

**Figure 4**

**A.**

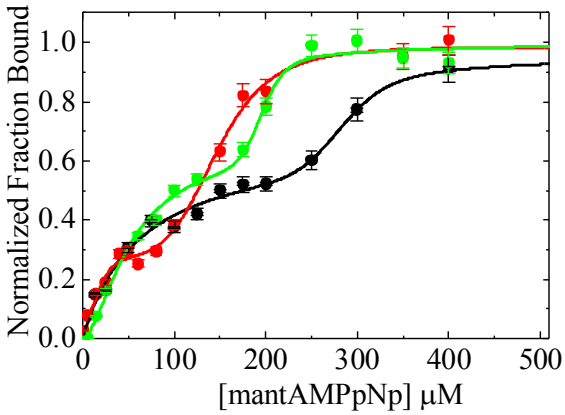


**B.**

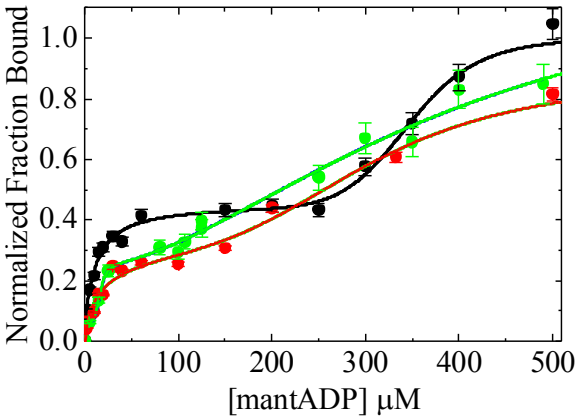


**C.**

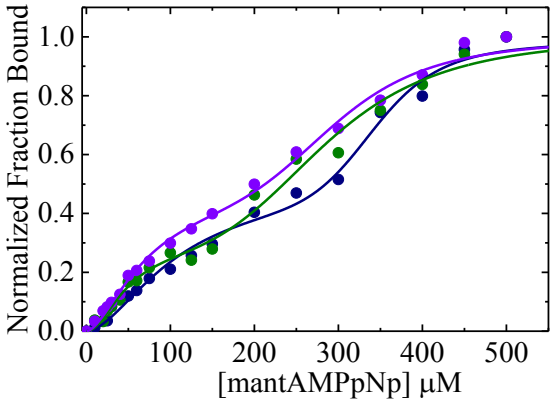


**D.**

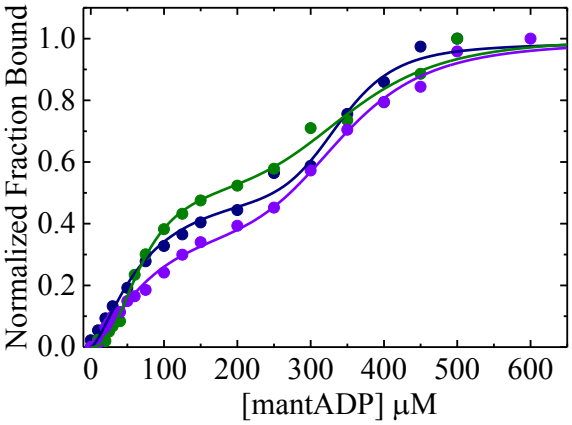

**Figure 5**